International Journal of Ocean Engineering and Technology Vol. 4, No. 1, pp 10~21, April 2001 (ISSN 1229-1668)

Sea Surface Statistical Properties as Measured by Laser Beam Reflections

KWI-JOO LEE*, YOUNG-SIK PARK* AND K. I. VOLIAK**
* *Department of Naval Architecture and Ocean Engineering, Chosun University*
** *Wave Research Center, General Physics Institute, Russian Academy of Science*
(Received 20 February 2001, accepted 30 March 2001)

ABSTRACT: *A new method of laser remote sensing is proposed, based on sensing the sea surface by a narrow laser beam (2-3cm) and analyzing statistically specular reflections. Construction of the angular dependency of the average density of specks versus the aircraft flight horizontal azimuth allows calculation of both intensity and azimuthal properties of the sea surface spectrum. The paper contains the experimental setup and technique, the field measurement data taken onboard an aircraft and the examples of calculated main statistical parameters of sea waves. Their energy-carrying component velocity is found by the mean velocity of an ensemble of specular points at the random sea surface. The surface wave nonlinearity is shown to affect substantially the statistical characteristics measured: mean numbers of specular areas with the given elevation and given slope, arranged along the line of crossing the sea surface by the scanning laser beam. Experimental measurement of a variance in the number of these areas yields a principal possibility to calculate the correlation function of the sea surface without its preliminary modeling.*

KEY WORDS: Wave Spectrum, Laser beam reflection, Sea surface.

1. Introduction

In the two last decades, laser methods have been developed for studying the sea waves, along with conventional techniques of air photography, contact measurement, and microwave backscattering. The laser active remote sensing has a number of advantages. Application of lasers, similar to radars, does not require uniform sea surface illumination, which facilitates the field experiments. Laser location from an aircraft allows investigation of vast surface areas for such a short time that the synoptic conditions cannot vary the sea state.

Currently, two basic techniques for laser remote sensing of the sea surface are commonly used: pulsed location and phase profilometry. The former method is based on measuring a delay between laser pulses probing and reflected from the sea surface, as well as on detecting the reflected pulse shape and duration (see for example (Stamm, 1973)). Such measurements are employed to find the mean level and slope of the disturbed sea surface and to estimate the sea state. An accuracy of the mean sea level measured in a laser footprint is limited by the probing pulse duration.

Some remote technique developed presupposes illumination of the sea surface by short laser pulses incident at grazing angles (Gurevich, 1979a; 1979b). In each laser shot the probing pulse of duration τ illuminates a surface strip of length $c\,\tau$, where c is the speed of light. As the light pulse propagates, such a strip moves over the sea surface, yielding the signal reflected by areas oriented normally to the laser beam axis.

The analysis of a one-dimensional sea surface, carried out in the works (Gurevich, 1979a; 1979b), allows in principle establishment of an integral correlation between the reflected signal shape and the surface profile. Attempts have been undertaken also to find the correlation between the return signal shape and the reflecting surface parameters for vertical laser remote sensing. Under the condition of periodic illumination of the sea by light pulses with a spatial extent shorter than the characteristic length of surface waves, their temporal evolution seems to be traced too. Such an attempt was made in (Gurevich, 1976) when sounding the sea surface at grazing angles from a stationary platform.

Another method of pulsed remote sensing consists in the determination of sea wave statistical parameters by simultaneously illuminating large surface areas. For example, the results of vertical pulsed laser location were analyzed in (Goldin, 1979) where the variance of the sea surface heights was estimated by a temporal broadening of the reflected pulse.

When sounding quasivertically, the reflected signal hitting the receiver aperture is proportional to the probability of surface patches to have a normal coinciding with the source-to-receiver direction. This allows determination of the distribution of surface slopes, based on the dependence of the return intensity on the angle of laser beam incidence. The accuracy of such a technique used onboard an aircraft depends mainly on the reliable statistics of detected pulses and is improved with a higher laser repetition rate. This technique was qualitatively tested in (Pelevin, 1979) for the laser remote sensing from a shore.

Similar to(Goldin, 1979), the variance of sea surface slopes (on the assumption of their normal distribution) can be also measured by the temporal broadening of reflected signals at vertical incidence

of short pulses in a diverging laser beam (Ross, 1970; Kulyasov, 1979). There a few in number experiments have been carried out on the sea surface probing by short laser pulses from a helicopter. However, the horizontal resolution of laser remote sensing, controlled by the pulse duration, exceeds 3 m in all known implementations of this technique. This means that the method considered can be applied only to large-scale sea waves (with lengths of several tens of meters and amplitudes of order 1 m and higher). Therefore, the pulsed laser location has found no wide application for measuring the sea surface parameters.

In the surface phase profilometry one uses the laser phase rangefinder mounted onboard an aircraft and operating in the height measuring mode (Miller, 1965). Sequential readings of the sea height make it possible to reconstruct the surface profile along the flight direction. Schematics of such profilometers are well developed and were applied successfully to measure both land (Olsen, 1970; Lin, 1980) and sea (Voliak, 1986; Bunkin, 1987) surface profiles. However, measuring principles in these two cases differ substantially due to different mechanisms of the return. When sounding the land surface, light backscattering is pure diffusive, which maintains constancy (or at least variations in a narrow dynamic range) of the received signal. The sea return, as was indicated earlier, contains an intensive mirror component along with the diffuse backscattering component from the proper surface and the subsurface particles. Simultaneous reception of the reflected and scattered signals is technically difficult since the ratio of their intensities is 10^3-10^4 so that, under these conditions, the reflection plays the role of a powerful pulsed interference. Phase measurements of the sea surface profile by lasers yield data on a long-wave spectral range of the sea roughness, for example, on its spectral peak.

The goal of many oceanographic works is a study in both large- and small-scale sea waves. For example, there is the important problem of interaction between internal and surface waves, at which variations in the spectrum of short surface waves are most significant. Therefore, it is urgent to develop a laser method for measuring parameters of the sea roughness with wavelengths from a few centimeters to several tens (or even hundreds) of meters.

In the present work we investigate the method for remote laser measurement of the sea wave statistical parameters, based on continuous sensing of the sea surface by a narrow laser beam and on reception of directly reflected signals (see (Bunkin, 1985; Solntsev, 1986)). The high beam directionality allows the resolution of sea areas of order of few centimeters squared and the study of small-scale surface waves. Optical location of the sea surface by mirror-reflected signals allows also implementation of the above advantages of the laser as a remote sensing instrument.

The data on surface waves are extracted as follows. The reflected signal at the lidar receiving system input represents a random sequence of light pulses corresponding to the probing beam hitting a surface patch with the quasispecular slope. As distinct from the laser phase profilometry, the proposed technique yields no information on a concrete sea surface profile along the beam scan (aircraft flight). However, taking the surface wave randomness into account, such data are not always necessary since only statistical parameters of the sea surface are of interest. In our technique, the probabilistic analysis of the random sequence of mirror-reflected laser specks allows determination of the wave statistical properties. In particular, experimental measurement of the azimuthal function for mean density of such specks when scanning over the sea surface at various directions enables one to estimate both angular parameters of the energy spectrum and a surface wave state in terms of its development and saturation.

In the present work we propose a technique for calculating statistical parameters of the laser speck sequence, taking surface wave motion into account, and analyze experimental data on oblique remote sensing of the sea surface with corresponding corrections.

The random surface is usually described by the Gaussian statistics of a linear ensemble of surface waves. However, such an approach is applicable to a rather weak sea roughness when the surface slopes are small. To describe statistical properties of the well-disturbed sea surface, nonlinear corrections should be considered also. The model of a random nonlinear wavepacket, based on the Stokes expansion (Longuet-Higgins, 1957), is quite pictorial and allows a detailed study of various sea wave statistical parameters. Based on such one-dimensional model of a nonlinear random wave field, we will study these parameters measured by remote sensing with a narrow laser beam: the mean density of beam crossings with a given sea level and the mean number of surface points with a given slope per unit length.

The paper is organized as follows. In Sec. 2, we outline the laser remote sensing model, as well as a procedure for extracting sea wave data by the mean density of specks reflected along a flying laboratory route. Section 3 presents the results of field experiments and the numerical calculations of sea spatial energy spectrum. Section 4 is dedicated to derivation of a differential equation for determining the correlation function of sea surface based on an experimentally determined variance in the number of mirror-reflection points per a given length. In Sec. 5, we develop the technique for calculating the statistical parameters of a laser speck sequence received from the moving sea surface and analyze the experiments on oblique remote sensing taking the calculated corrections into account. Section 6 is devoted to an analysis of the impact of gravity surface wave nonlinearity on such experimentally measured wave parameters as the mean number of crossings with a given level and the mean density of points with a given slope at the random sea surface.

2. Model of Mirror-reflection Speck

The experimental layout is shown in Fig. 1. A narrow laser beam from a horizontally flying platform is directed onto the sea surface at a nonzero angle to the vertical. (The unperturbed free surface level is accepted as a horizontal plane.) We characterize the laser beam position by two angles γ' and β' (see Fig. 1) that can be interpreted also as the platform pitch and roll, respectively.

The platform moves rectilinearly and uniformly along the axis x'. As was indicated in introduction, the laser location from the high-speed platform (aircraft) allows exploration of vast surface areas for a short time, during which synoptic conditions cannot change. This allows us to accept the hypothesis of "frozen" surface: $\xi = \xi(x, y)$, where ξ is the sea surface elevation and (x, y) is a certain immobile frame of horizontal Cartesian coordinates. (Below in Sec. 7 we consider also corrections for the impact of sea surface motion on the wave statistical properties.)

Let the beam motion plane form an angle θ with the axis x and be defined by the equation $x \sin\theta - y \cos\theta = 0$. This plane crossing with the sea surface defines a random trajectory of the light footprint. In the plane (x, y), we introduce coordinates (x', y') in the direction of θ and perpendicular to it,

$$x' = x\cos\theta + y\sin\theta, \qquad y' = -x\sin\theta + y\cos\theta. \tag{1}$$

Then the curve of beam-sea crossing can be written as $\zeta = \zeta(x')$. Spikes in the received signal correspond to the curve ζ points where the surface has a quasispecular slope.

To describe the experiment, quasispecular conditions should be defined, that is the conditions when the receiver aperture is hitted by a reflected signal of power no lower than a prescribed value. The study (Rice, 1944) shows that the quasimirror reflection conditions are controlled by the experimental geometry (flight altitude H, receiving diaphragm size d and shape S, light beam radius a, and surface curvature $\varkappa$ at the incident beam axis) and the instrumental noise. The basic dimensionless parameters defining these conditions are $\alpha_i = d/4\,\varkappa_i\, aH$, where $\varkappa_i$ $(i = 1, 2)$ are surface principal curvatures at the laser footprint center.

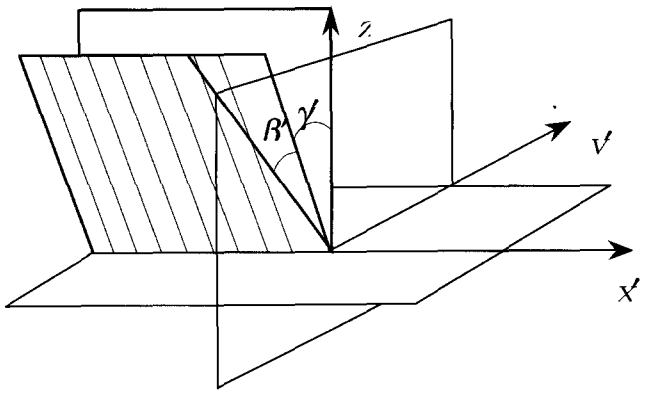

Fig. 1 Schematic of laser remote sensing

We write the conditions defining the quasispecular surface areas (points) in the form

$$\zeta_{x'} = \beta, \qquad \zeta_{x'} \in (\gamma - \alpha, \gamma + \alpha), \qquad \beta = \tan\beta', \qquad \gamma = \tan\gamma', \tag{2}$$

where γ' and β' correspond to pure specular reflection from the sea surface, the small allowed deviation α is controlled by the spatial shape of the reflected signal, as well as by the receiver noise. Estimates show that the parameter α is of order 10^{-2}.

Quasispecular conditions (2) satisfy, for example, the inequalities $\alpha_{1,2} << 1 << \alpha_{2,1}$ for any receiving diaphragm shape. An oceanographic example of such a case is a sufficiently anisotropic sea with the narrow directional surface wave energy spectrum $E(u, v)$:

$$(m_{20} + m_{02})\left(m_{02}m_{20} - m_{11}^2\right)^{-1/2} >> 1, \tag{3}$$

where

$$m_{ij} = \int\int u^i v^j E(u, v)\, du\, dv \tag{4}$$

are moments of the two-dimensional spectrum and (u, v) are components of the wavevector k. Laser sounding in the near range (Rice, 1944) corresponding to the criterion $\alpha_{1,2} >> 1$ also satisfies conditions (2) if a receiving slit diaphragm is arranged normally to the aircraft flight direction.

Mirror reflection points lying at the cutting curve $\xi = \xi(x')$ represent a random sequence characterized by the mean number and variance of laser specks and by the higher moments of that number within a given length. The distributions of distances between sequential specks and of a reflected signal intensity controlled by the surface curvature at the reflection point are also of importance. Statistical analysis of the speck sequence carries rich information on the spatial energy spectrum and the surface correlation function.

3. Mean Density of Laser Specks

First, we consider the mean number (or density) $N(\theta)$ of specks per unit length of the curve $\zeta = \zeta(x')$. On the assumption of a steady random surface, the above density is given by

$$N=\int_{\gamma-\alpha}^{\gamma+\alpha} d\xi_{y'}\int_{-\infty}^{\infty} P\left(\xi_{x'}=\beta,\xi_{y'},\xi_{x'x'}\right)\left|\xi_{x'x'}\right| d\xi_{x'x'}. \tag{5}$$

For the Gaussian random field it can be written in the final form:

$$N(\theta)=\frac{1}{2\pi}\left(\frac{m_4(\theta)}{m_2(\theta)}\right)^{1/2}\exp\left(-\frac{\beta^2}{2m_2(\theta)}\right)\left\{\operatorname{erf}\left[(\gamma+\alpha)\left(\frac{m_2(\theta)}{2\Delta_2}\right)^{1/2}\right]-\operatorname{erf}\left[(\gamma-\alpha)\left(\frac{m_2(\theta)}{2\Delta_2}\right)^{1/2}\right]\right\}, \tag{6}$$

where erf(·) is the error function, $\Delta_2=m_{20}m_{02}-m_{11}^2$, is the surface $\xi(x, y)$ invariant relative to rotation of the frame of reference, and $m_n(\theta)$ are nth moments of the energy spectrum of curve $\zeta(x)$, which can be expressed via the moments of two-dimensional energy spectrum of the surface $\xi(x,y)$ (see(Jansen, 1984)) as

$$m_2(\theta)=m_{20}\cos^2\theta+2m_{11}\cos\theta\sin\theta+m_{02}\sin^2\theta,$$
$$m_4(\theta)=m_{40}\cos^4\theta+4m_{31}\cos^3\theta\sin\theta+6m_{22}\cos^2\theta\sin^2\theta+4m_{13}\cos\theta\sin^3\theta+m_{04}\sin^4\theta. \tag{7}$$

The invariant Δ_2 is a measure of the surface wave two-dimensionality. In the limit $\Delta_2\to 0$, formula (6) yields the known result of (Phillips, 1966) for the one-dimensional case:

$$N=\frac{1}{\pi}\left(\frac{m_4}{m_2}\right)^{1/2}\exp\left(-\frac{\beta^2}{2m_2(\theta)}\right). \tag{8}$$

In another limit ($\alpha\to 0$), the mean density of specks along the curve $\zeta(x)$ is finite only at the nonzero ratio $\alpha/\Delta_2^{1/2}$, that is at a rather weak two-dimensionality of the surface.

An experimental determination of $N(\theta)$, for example, at strictly vertical sounding of the sea surface ($\beta=0$, $\gamma=0$) makes it possible to find all the second and fourth moments of two-dimensional energy spectrum $E(u, v)$ as follows. Substituting (7) into formula (6) for $N(\theta)$, one finds a functional equation with the scanning direction θ as an independent variable. Its left-hand side includes the experimentally measured function $N(\theta)$ while the right-hand side contains the function θ of a specified analytical form with undetermined coefficients depending only on the second and fourth moments.

The optimum approximation of function $N(\theta)$ by analytical form (6) allows determination of the energy spectrum moments. As a computing procedure, the least squares method can be used to find the moments entering Eqs. (7).

In turn, the two-dimensional energy spectrum parametrization (accepted in physical oceanography, see (Cramer, 1976)) in a specified analytical form allows determination of the whole set of the spectrum parameters by the moments found. The proposed technique provides for selection and determination of at least eight such parameters. A basic feature of the approach is the possibility to study the azimuthal dependence of the wave energy spectrum in detail, which remains not adequately studied up to now.

We analyze the dependence of the mean number $N = N(\theta)$ of specular reflection points on various sea wave characteristics, parametrizing the spatial energy spectrum of sea surface elevation as

$$E(k,\theta)=\begin{cases}\dfrac{Ak_0^{1/2(m-5)}k^{-1/2(m+3)}\left(g+\cos^{2n}\theta\right)}{g+1} & \text{at } k_0\le k\le k_1,\\ 0 & \text{at } k<k_0,\ k>k_1.\end{cases} \tag{9}$$

Two-dimensionality of spectrum (9) is specified by the isotropy parameter g and the angular parameter n = 0, 1, 2,... The spectrum saturation depends on the number m: m = 5 and m > 5 correspond respectively to the saturated Phillips spectrum and to still developing waves; and the constant A is $6\cdot 10^3$ (Steiberg, 1966). The wavenumbers k_0 and k_1 can be found experimentally from the distribution of times between neighboring specks: k_0 and k_1 are inversely proportional respectively to the maximum and minimum scales of the distribution features. The direction θ=0 in (9) coincides with the wind speed vector (θ=0 and $\pi/2$ are principal axes of the spatial spectrum $E(k, \theta)$).

Calculating the spectrum (9) moments, from (6) and (7) one readily finds the function $N = N(\theta)$ taking the realistically small reception aperture α << 1 into account,

$$N(\theta)=F\left[(1+g)\frac{m_{40}\cos^4\theta+6m_{22}\cos^2\theta\sin^2\theta+m_{04}\sin^4\theta}{m_{02}m_{20}}\right]^{1/2}, \tag{10}$$

where

$$m_{ij}=2\Gamma\left(\frac{j+1}{2}\right)\left(g\frac{\Gamma\left[(i+1)/2\right]}{\Gamma\left[(i+j)/2+1\right]}+\frac{\Gamma\left[(i+1)/2+n\right]}{\Gamma\left[(i+j)/2+n+1\right]}\right), \tag{11}$$

$$F=\begin{cases}\dfrac{\alpha}{\left(\pi^3A\right)^{1/2}}k_0^{(m-5)/4}k_1^{1-(m-5)/4}\dfrac{m-5}{1-\left(k_0/k_1\right)^{(m-5)/2}}\left(\dfrac{1-\left(k_0/k_1\right)^{(9-m)/2}}{9-m}\right)^{1/2}, & m\neq 5,\\ \dfrac{\alpha}{\left(\pi^3A\right)^{1/2}}k_1\dfrac{\left[1-\left(k_0/k_1\right)^2\right]^{1/2}}{\ln\left(k_1/k_0\right)}, & m=5.\end{cases}$$

One readily sees from (10) that the expression in brackets defines the azimuthal dependence $N(\theta)$ while the function F in (11) specifies properly the speck density scale.

4. Numerical Calculation of the Speck Density

The spectrum angular and isotropy parameters, n and g, totally define the azimuthal shape of $N(\theta)$ (see (10)). Figure 2 displays

the calculated angular dependence of the number of specks per unit length for the saturated spectrum (m = 5) and various n (the value g is put to zero). For all n the function $N(\theta)$ has two symmetric maxima arranged along the wind speed vector, as well as two minima in the orthogonal direction. As the number n increases, the angular dependence $N(\theta)$ becomes increasingly pronounced. For all $n \neq 0$ and g = 0 this dependence is dumbbell-like. As the spectrum isotropy (that is g) grows, the function $N(\theta)$ becomes convex upward at all points.

Figure 3 shows dependencies of the ratio $\delta = N_{min}/N_{max}$ of principal semiaxes for the distribution $N(\theta)$ on the isotropy parameter g at various spectrum angular parameters n. At n = 1 and 2 the value δ grows almost linearly with the isotropy parameter g, asymptotically approaching unity at large g. As the angular directionality n increases, the ratio of principal semiaxes quickly drops at $g \leq 0.5$ while for g > 0.5 the value n has no appreciable impact on the ratio δ.

The order of magnitude of the speck density is defined by the set of spectral parameters A, m, k_1, and k_0. The calculations show that various wave motion scales have a significant impact on that density at a saturated sea with m = 5. In particular, short surface waves with $k \sim k_1$ substantially contribute into the statistics of "mirror" points.

For unsaturated seas defined by m > 5 (a narrower energy spectrum), the impact of the long-wave spectral range is more

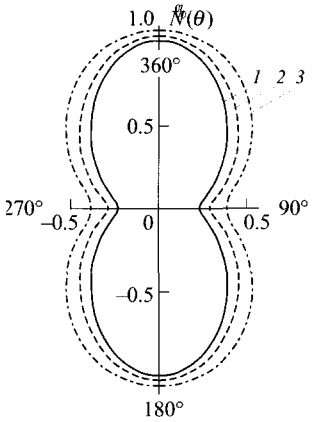

Fig. 2 Angular dependence of the normalized mean number of speck per unit length

$$N(\theta) = N(0)\, F[(1+g)m_{40}/m_{20}m_{02}]^{1/2-1}$$

at n=1 (*1*), 2 (*2*), and 3 (*3*); m=5 and g=0

substantial, and the speck density at m = 9 is mainly controlled by the long-wave components of the surface spectrum ($k \sim k_0$).

5. Flight Investigation of Sea Waves: Statistics of Laser Reflection Specks

5.1 Experimental

The flight experiments on detection of specular reflexes from the rough water surface were carried out onboard an Antonov-30 aircraft at the Black Sea in 1980s. Some ranges of the experiments are shown in Fig. 4. The flight altitude was 330 m and the aircraft speed was varied from 280 to 320 kmh-1 depending on wind velocity and direction. The trajectory of flights aimed to measure angular dependencies of laser speck statistics represented a star of 12 straight tacks (see Fig. 5) of length 10 km. The total time of flight over the whole star route was about 40 min.

Data arrays corresponding to various Black Sea areas and weather conditions had been accumulated during the experiments. Each series consisted of 12 tack records and allowed establishment of statistical sea properties in an explored range.

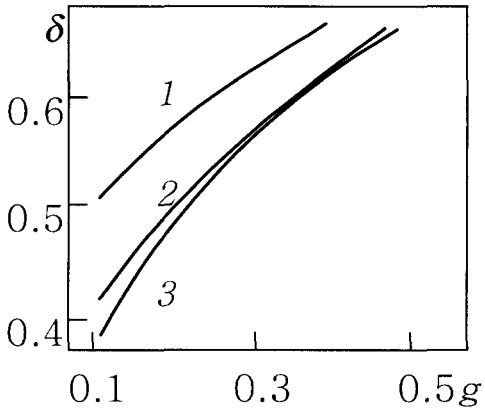

Fig. 3 Dependence of the ratio $\delta = N_{min}/N_{max}$ of principal semiaxes of the distribution N(θ) on the isotropy parameter g. Number at curve are the spectrum angular parameter n.

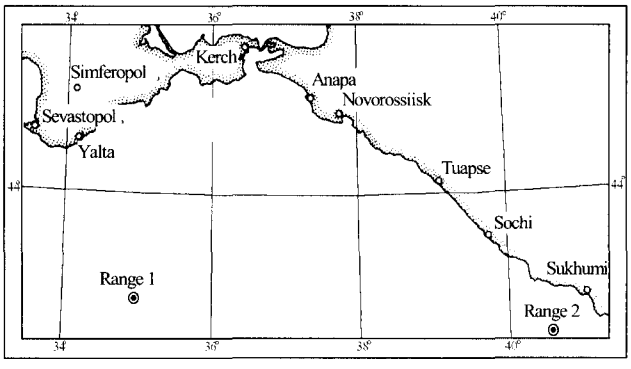

Fig. 4 Field experiment ranges.

The measured data were preliminarily processed immediately during the experiment using an onboard computer. Final processing with necessary corrections was carried out on the land with the use of a tape recorder.

The distributions of speck intensity and mean density, as well as of spacing between neighboring specks were calculated by experimental records in each run for all 12 tacks of the flying laboratory. The experimental conditions of some runs are listed in Table 1.

5.2 Data

The measured mean densities $N(\theta)$ of laser specks from the sea surface are shown in Fig.6 as identically oriented with respect to the wind velocity. As was expected, the curves $N(\theta)$ have maxima in directions along and against the wind velocity and minima in the orthogonal direction.

Experimental points of run 5 (see Fig. 6) are arranged almost over a circle, indicating respectively almost the total sea wave isotropy. The data of run 2 form a dumbbell-shaped contour,

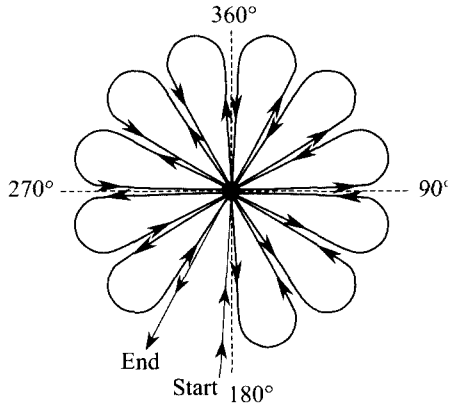

Fig. 5 Flight trajectory during field experiments

demonstrating the narrow directionality of wind wave spectrum. The run 3 points form also a similar but larger dumbbell, seemingly caused by stronger narrowly directed waves that develop under a durable wind action.

To interpret adequately the experimental data, free parameters of the spatial energy spectrum of sea waves, given in the form of (9), were numerically calculated by the above technique.

The results are shown in Fig. 6 by three curves. Curve *5* approximating the dependence $N(\theta)$ in run 5 corresponds to the isotropic developed sea with $n = 0$ and $m = 5$. Curve (run) *2* corresponds to the narrow spectrum of developed surface waves having $n = 3$, $m = 5$, and $g = 0$. Points of run 3 appears close to curve *3* with $n = 2$, $m = 5$, and $g = 0.13$, reflecting a sufficiently narrow directionality of the developed sea having also a certain isotropic component.

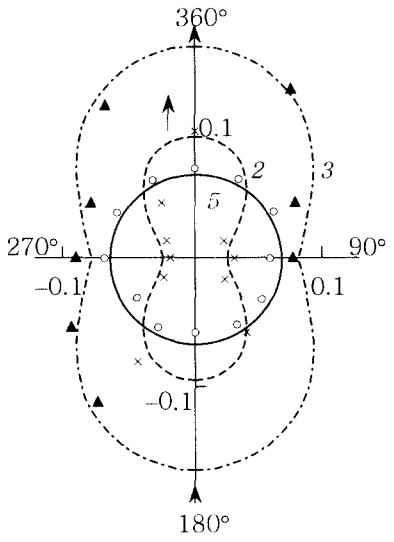

Fig. 6 Experimental and calculated dependencies $N(\theta)[m^{-1}]$ for various field experiment runs presented in Table 1. Indices near curves correspond to the run numbers.

Table 1 Experimental conditions.

Run	Range	Date	Local time	Meteoconditions	Sea state
1	2	May 29, 1984	18:50-19:30	Cloudy	Appreciable swell (300°)
				Wind 200°	crossing the wind waves
2	1	May 30, 1984	12:00-12:40	Clear	Developed sea
				Wind 150°	
3	2	May 30, 1984	13:30-16:10	Cloudy	Developed sea,
				Wind 300°	wave direction is 300°
4	1	June 12, 1984	8:00-8:40	Clear	Wind waves of 12 balls
				Wind 240°	by Beaufort
5	1	June 14, 1984	18:30-19:10	Clear	Visually isotropic sea
				Wind 270°	

The possibility shown for a consistent approximation of the numerically simulated spatial wave spectrum to the data of aircraft laser experiments confirms applicability of the developed technique for determining the spectrum parameters by statistics of direct reflection specks from the sea surface. The visual observation data of Table 1 quite conform to the above analysis.

However, such a technique is not always applicable. For example, two systems of surface waves propagating at an angle to each other were observed visually in run 1: wind waves and a swell caused supposedly by a remote storm. The experimental azimuthal function $N(\theta)$ of that run is plotted in Fig. 7.

Four maxima and a general irregularity of the dependence confirm the existence of two crossed wave systems. In this case, the spatial spectrum of form (6) is inapplicable, and the correlation function of the sea surface should be numerically calculated by the higher moments of distribution, found for the speck random sequence.

6. Variance in the Number of Specular Points. Correlation Function of a Random Surface

The mean number N of quasispecular points per unit length of the sea surface section $\zeta = \zeta(x)$ is the simplest characteristic of the random sequence of laser specks. The variance in the number of surface points with a given characteristic within the interval of a fixed length yields a significant data array on the correlation function of sea surface waves.

First, we consider a one-dimensional frozen wave field. Then, if the random process $\zeta = \zeta(x)$ is Gaussian and steady, the kth factorial moment of the number of mirror points, where $\zeta_x = 0$, on the interval $(0, X)$ is given by (see(Longuet-Higgins, 1963))

$$M_k(X) = \int_0^X \cdots \int dx_1 \cdots dx_k \int_0^\infty \cdots \int |y_1 \cdots y_k| P_x(u, Y)\, dy_1 \cdots dy_k, \tag{12}$$

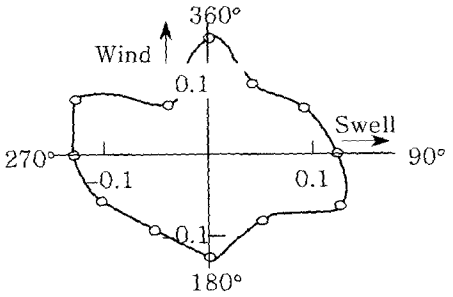

Fig. 7 Experimental dependence $N(\theta)$[m^{-1}] for two systems of surface waves directed at an angle to each other

where $y_i = \partial^2 \zeta / \partial x^2$ $(x = xi)$; $P_x(u,Y) = P_x(0, \ldots, 0, y_1, \ldots, y_k)$ is the joint density of probabilities for randoms $\zeta_x(x_1)$ ... $\zeta_x(x_k)$ and $\zeta_{xx}(x_1)$ ... $\zeta_{xx}(x_k)$, taken at the points x_1 ... x_k.

In particular, the variance D in the number of specks on the interval $(0, X)$ can be written as (see (Taifun, 1980))

$$D(X) = NX - N^2X^2 + 2\int_0^X (X - x)\Psi(x)\, dx, \tag{13}$$

where

$$\Psi(x) = \int\int_{-\infty}^{\infty} |\xi_{xx_1}\xi_{xx_2}| P\left(\xi_{x_1} = 0, \xi_{x_2} = 0, \xi_{xx_1}, \xi_{xx_2}\right) d\xi_{xx_1} d\xi_{xx_2}, \tag{14}$$

$\xi_{xx_i} = \xi_{xx}(x = x_i)$, $\xi_{x_i} = \xi_x(x = x_i)$, x = $x1$ - $x2$, and N is as before the mean density of specks per unit length.

Let us determine experimentally and represent the variance $D(x)$ by a sufficiently smooth function. Then, after twofold differentiation of both sides of (13) with respect to X and some algebra, we find

$$\Psi(X) = N^2 + \frac{1}{2}\frac{d^2}{dX^2} D(X). \tag{15}$$

The function $\Psi(X)$ (14) can be expressed via derivatives $r^{(}x) = \overline{\xi_x(x_1)\xi_x(x_1 + x)}\, m_2^{-1}$ of the correlation coefficient rx and via factorial moments $M_k(X)$ as

$$\Psi(X) = \frac{1}{\pi^2}\frac{\left(M_{33}^2 - M_{34}^2\right)^{1/2}}{\left[1 - r^{(}X)\right]^{3/2}}\left\{1 + \frac{M_{34}}{\left(M_{33}^2 - M_{34}^2\right)^{1/2}} \tan^{-1}\left[\frac{M_{34}}{\left(M_{33}^2 - M_{34}^2\right)^{1/2}}\right]\right\}, \tag{16}$$

where M_{ij} is the cofactor of element ij of the matrix

$$\Lambda = \begin{Vmatrix} 1 & r''(X) & 0 & r'''(X) \\ r''(X) & 1 & -r'''(X) & 0 \\ 0 & -r'''(X) & m_4/m_2 & -r^{IV}(X) \\ r'''(X) & 0 & -r^{IV}(X) & m_4/m_2 \end{Vmatrix}.$$

Where $\| \|$ represents the norm of the matrix, Thus, the set of Eqs. (14), (15) is reduced to the ordinary second-order differential equation for the function $r''(X)$ which can be solved numerically if the right-hand side of (15) is known.

Taken the boundary conditions $r(0) = m_0/m_2$, $r'(0) = r'''(0) = 0$, and $r''(0) = 1$ into account, the correlation function can be calculated to within the normalizing factor m_0, that is the root-mean-square surface elevation.

For the two-dimensional surface waves, Eq. (15) is written as

$$\Psi\left(X', Y' = 0\right) = N^2(\theta) + \frac{1}{2}\frac{d^2}{dX'^2} D\left(X', 0\right), \tag{17}$$

where $N(\theta)$ is the mean density of specks per unit length along the random curve $\zeta = \zeta(x')$ constructed by the surface crossing with the scanning plane $x\sin\theta - y\cos\theta = 0$ and $D(X', \theta)$ is the variance in number of quasispecular points on the interval $(0, X')$ of this curve. Then function (16) is given by

$$\Psi(X', Y'=0) = \int_{-\alpha}^{\alpha} d\xi_{y'1} \int_{-\alpha}^{\alpha} d\xi_{y'2} \int\int_{-\infty}^{\infty} |\xi_{x'x'_1}\xi_{x'x'_2}| P(\xi_{x'1}=0, \xi_{x'2}=0, \xi_{y'1}, \xi_{y'2}, \xi_{x'x'1}, \xi_{x'x'2}) d\xi_{x'x'1} d\xi_{x'x'2}, \tag{18}$$

where α is the earlier estimated utmost surface slope defining the interval of specular reflection,

$$\xi_{x'x'_i} = \xi_{x'x'}(x' = x'_i), \quad \xi_{x'_i} = \xi_{x'}(x' = x'_i), \quad \xi_{y'_i} = \xi_{y'}(x' = x'_i). \tag{19}$$

Function (18) can be expressed in terms of second-, third-, and fourth-order derivatives for the time correlation function

$$R(x', y') = \overline{\xi(x_1 + x', y_1 + y')\xi(x_1, y_1)} \tag{20}$$

over coordinates x and y.

After returning to the initial frame of reference (x, y), Eq. (17) becomes a nonlinear fourth-order equation in partial derivatives with respect to the correlation function $R(x, y)$, which can be also a basis of numerical calculations. The right-hand side of (17) should be found by experimental data processing.

Implementation of the proposed method for determining the sea wave correlation function will be subject of an independent study.

7. Statistical Properties of the Moving Sea Surface

The above statistical calculations of laser specks from the sea surface are based on the approximation of frozen sea, which is justified at high carrier speeds $vc >> c$, where c is the characteristic (phase) velocity of surface waves. Actually, for example in the experiments (Grigoriev, 1987; Huang, 1980), the speed of the aircraft with a laser wavemeter aboard is $vc \sim 100$ m · s^{-1}, thus the large-scale wave velocity $c \sim 10$ m · s^{-1} can be an appreciable fraction of the carrier speed.

In this section we propose the technique for calculating statistical characteristics of the laser speck sequence taking surface wave motion into account and analyze the data on oblique laser remote sensing of the sea surface considering the corresponding corrections.

As was shown above, in the case of oblique sounding of the statistically uniform Gaussian surface by a narrow laser beam during circular flights, the azimuthal dependence of the mean density of specks per unit length of the circular scan should be a dumbbell-like curve extended in the direction of surface wave (wind) propagation. The curve is symmetrical relative to principal axes of the spatial spectrum. The density of specks in these (frozen) axes is given by

$$N_f = 4D\exp\left(-\frac{\xi_x^2 m_{02} + \xi_y^2 m_{20}}{2m_{02}m_{20}}\right), \tag{21}$$

where D is the mean density of zero slope points per unit area of the surface $\xi = \xi(x, y)$, ξ_x and ξ_y are slope components at the surface mirror points, and m_{ij} are moments of the spatial energy spectrum of surface ξ.

An example of experimental azimuthal dependencies for such oblique remote sensing is given in Fig. 8 by the curve *a*. The experiments were performed at the Black Sea in an area with coordinates 42°N 40°E. The flight trajectory represented a star of 12 straight tacks 10 km long, the mean aircraft speed was vc = 83 m · s^{-1}, and the roll was 4°. As is evident from Fig. 8, the symmetry center of the experimental curve *a* was displaced in the upwind direction.

The experiments were also carried out at the Pacific in an area with coordinates 53°N 158°E for aircraft rolls of 10° and 5°. The experimental azimuthal dependence for the 10° roll is shown in Fig. 9 by curve *a*. The axis x of the frame of reference in the figure coincides with the wind direction. It is evident that symmetry axes x^0 and y^0 of the constructed experimental curve were turned by the angle $\varnothing$ relative to the coordinate axes and even the symmetry center is displaced appreciably toward the axis x..

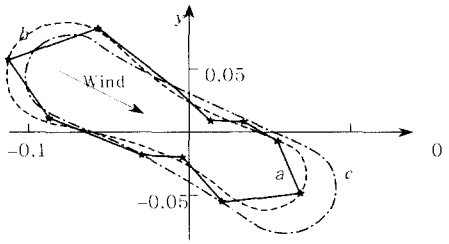

Fig. 8 Azimuthal dependence of the mean density [m^{-1}] of speckular points in the Black Sea experiment : experimental data(a), curve calculated taking the specular point motion into account (b), and data calculated by the surface model (c).

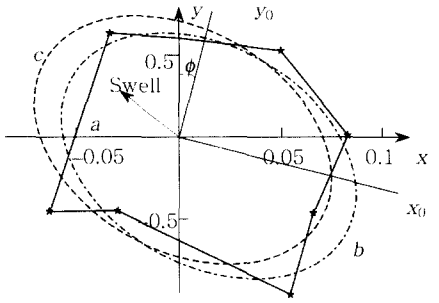

Fig. 9 Same as in Fig 8. for the Pacific experiment

We note that in the approximation of "frozen" sea surface the curve $N_3 = N(\theta)$ should have the symmetry center and axes coinciding to principal axes of the random surface. The account of surface motion allows explanation of the curves $N(\theta)$ found experimentally.

We estimate the impact of surface motion on experimentally measured values. For simplicity, we consider a one-dimensional case. The experimentally measured mean number of mirror points per unit length is a flow of such specks per unit time, which can be written as

$$W = \int_{-\infty}^{\infty}\int_{-\infty}^{\infty} vp(\xi_x, \xi_{xx}, v)|\xi_{xx}|d\xi_{xx}dv, \tag{22}$$

where v is the velocity of a mirror-reflection point, determined by relationships

$$0 = d\xi_x = \xi_{xx}dx + \xi_{xt}dt, \qquad v = \frac{dx}{dt} = -\frac{\xi_{xt}}{\xi_{xx}}, \tag{23}$$

and $p(\xi_x, \xi_{xx}, v)$ is the joint probability density of values ξ_x, ξ_{xx}, and v.

For the Gaussian surface, one writes

$$p(\xi_x, \xi_{xx}, v) = p(\xi_x)\, p(\xi_{xx}, v) = \frac{\exp\left(-\xi_x^2/2m_2\right)}{\left(2\pi m_2\right)^{1/2}} p(\xi_{xx}, v). \tag{24}$$

After integration, we have

$$W = \frac{m_3'}{\pi m_4^{1/2} m_2^{1/2}} \exp\left(-\frac{\xi_x^2}{2m_2}\right), \tag{25}$$

where

$$m_{2p} = \overline{\left(\frac{\partial^p \xi}{\partial x^p}\right)^2}, \qquad m_q' = \overline{\left(\frac{\partial^q \xi}{\partial x^q}\right)\frac{\partial \xi}{\partial t}}. \tag{26}$$

The number of laser specks per unit length for the frozen surface and their mean velocity are given by (see (Jansen, 1984))

$$N_f = \frac{1}{\pi}\left(\frac{m_4}{m_2}\right)^{1/2} \exp\left(-\frac{\xi_x^2}{2m_2}\right), \tag{27}$$

$$\overline{V} = \frac{m_3'}{m_4}. \tag{28}$$

Comparing (25), (27), and (28), one finds $W = N_f \overline{V}$. Thus, the experimentally measured density of specks is equal to that density for the frozen surface, multiplied into the mean velocity of mirror points relative to an immobile optical receiver. Analogous considerations are valid also for the two-dimensional case.

In the experiments one has $\overline{V} = V_C + C_\theta$ where c_θ is the projection of the mean velocity of mirror points onto the flight direction. Hence, one finds $N = N_f (v_c + c_\theta)$. To determine the wave phase velocity c, we compare the experimentally measured values N in opposing directions N_{al} and N_{op} and find the values c_θ^e for each azimuth as $c_\theta^e = v_c(N_{op} - N_{al})(N_{op} + N_{al})^{-1}$. The wave direction $\varnothing$ and velocity c are calculated by the least squares method. Then we calculate the second moments m_{ij} $(i + j = 2)$ of the two-dimensional surface energy spectrum by (Jansen, 1984) and (Phillip, 1966). Based on the found values of c and m_{ij}, we construct approximating curves b for $N(\theta)$ (see Figs. 8 and 9). For comparison, these figures also depict corresponding curves c calculated within the frozen surface model.

The calculation by the experimental data of Fig. 8 yields the mean velocity of mirror specks as c = 10.6 m · s^{-1}. This qualitatively corresponds to the pure wind waves observed visually. The velocity c can be related to the phase velocity of an energy carrying peak of the sea wave spectrum.

Figure 9 display the experimental data and calculated curves corresponding to a more complicated oceanographic case when, along with wind waves, a supposedly stormy swell was observed at an angle to the wind direction. In this case, the mean surface velocity is oriented between the wind wave and swell directions. For the experiments with 10° and 5° rolls, the calculated mean velocities of surface mirror points were respectively c = 8.7 and 9.2 m · s^{-1} with directions $\varnothing$ = 14° and 11°; the moments were $m_{02} = 1.5 \cdot 10^2$ and $m_{20} = 1.8 \cdot 10^2$. The wave angular directionality factor $(m_{20}/m_{02})^{1/2} \approx 1.1$ is close to unity, which indicates quite an isotropic sea. The root-mean-square surface slope is $\sigma = (m_{20} + m_{02})^{1/2} \approx 0.2$, hence, the system of surface waves is saturated and virtually close to breaking.

The data found show that the difference between calculated mean velocities of surface mirror points and moments of the surface energy spectrum for the aircraft rolls 10° and 5° does not exceed 5 %, which confirms a correctness of the technique applied.

8. Nonlinear statistical parameters of the random sea surface

The above calculations assume that the Gaussian statistics is inherent in the sea surface. However, such an approach is applicable in fact at a rather weak roughness when the surface slopes are small. At a higher sea, nonlinear corrections should be taken into account to describe statistical properties of the surface waves.

Statistical models of the random sea surface with nonlinear interactions between spectral components were proposed

in(Longuet-Higgins, 1957) The account of nonlinearity in the model [27] calls for awkward numerics. The model of a random nonlinear wavepacket, based on the Stokes expansion (Longuet-Higgins, 1957), is quite pictorial and allows detailed studies of various surface wave parameters.

Assuming as before the one-dimensional model of a random wave field, we study the sea surface parameters that can be measured in a remote laser sensing experiment, that is the mean density N_{lev} of crossings of a given sea level and the mean number N_s of points of a given slope per unit length.

The narrow wavepacket of surface gravity waves is specified by the Stokes expansion with random parameters (see (Longuet-Higgins, 1957)) as

$$\xi = \frac{1}{2}a^2k + a\cos\chi + \frac{1}{2}a^2k\cos 2\chi + \frac{3}{8}a^3k^2\cos 3\chi + \mathrm{K}\ , \qquad (29)$$

where a is the wave amplitude, k is the wavenumber, n is the frequency, $\chi = kx - nt + \varnothing$ is the total phase, and $\varnothing$ is its initial value. The amplitude a is assumed to be a random continuously distributed value obeying the Rayleigh law, the phase $\varnothing$ is uniformly distributed over the interval [0, 2π]. We introduce the normalized randoms

$$z_1 = \frac{a\cos\chi}{\left(\overline{a^2}/2\right)^{1/2}},\quad z_2 = \frac{a\sin\chi}{\left(\overline{a^2}/2\right)^{1/2}},\quad h = \frac{\xi}{\sigma},$$

$$h_x = \frac{\xi_x}{\delta}\ \ (\delta = \sigma k),\quad h_{xx} = \frac{\xi_{xx}}{k\delta},\quad N = \frac{\sigma}{\left(\overline{a^2}/2\right)^{1/2}},\quad \sigma = \left(\overline{\xi^2} - \overline{\xi}^2\right)^{1/2}, \qquad (30)$$

$w\overline{(a^2)}^{1/2}$ is the root-mean-square value of a.

Since z_1 and z_2 are independent functions, their joint distribution is given by

$$p(z_1, z_2) = \frac{1}{2\pi}\exp\left(-\frac{z_1^2 + z_2^2}{2}\right). \qquad (31)$$

To calculate the mean density of points with the given level $h = h_0$, we invoke the formula derived in (Phillips, 1966)

$$N_{lev} = \int_{-\infty}^{\infty} p(\xi, \xi_x)_{\xi=\sigma h_0}|\xi_x|d\xi_x = \sigma^2k^2\int_{-\infty}^{\infty} p(h, h_x)_{h=h_0}|h_x|dh_x, \qquad (32)$$

where $p(\xi, \xi_x)$ and $p(h, h_x)$ are the joint probability distributions of values ξ, ξ_x, and h, h_x. The probability $p(h, h_x)$ can be written in the second order with respect to δ as (see (Longuet-Higgins, 1957))

$$p(h, h_x) = \frac{N^2}{2\pi k}(2k\sigma - 1)^2\exp\left\{-\frac{1}{2}N^2\left[\left(h - \delta h^2\right)^2 + \left(2\delta h h_x - h_x/k\right)^2\right]\right\}. \qquad (33)$$

Substituting (33) into (32) and integrating, one finds

$$N_{lev}(h_0, e) = \frac{k}{\pi}\exp\left[-\frac{1}{2}h_0^2\left(1 - 2\pi e h_0\right)^2\right], \qquad (34)$$

where $\delta = 2\pi e$ and $N = 1$ in the accepted approximation.

Dependence (34) has three extrema: maxima at points $h_{01} = 0$ and $h_{02} = 1/\delta$ and a minimum at $h_{03} = 1/2\delta$. However, the value h_{02} has no meaning since it is beyond the domain of applicability of the model since the utmost Stokes wave steepness obeys the condition $hk/2\pi < 1/4\sqrt{3} \approx 0.144$ (Longuet-Higgins, 1957).

Figure 10 shows dependencies $N_{lev}(h_0, e)$ for various e. It is evident that when $e = 0$, which corresponds to a linear Gaussian model of the wave field, the dependence $N_{lev}(h_0, e)$ is an even function of $h0$ since $N(h_0) = N(-h_0)$. This symmetry is violated for a nonlinear surface: at $h_0 > 0$ the mean density of level h_0 crossings exceeds the corresponding value in linear approximation. As the nonlinearity parameter e grows, that difference increases (see Fig. 10). The asymmetry observed experimentally in the dependence $N_{lev}(h_0, e)$ can be a criterion of the sea wave nonlinearity.

Now we consider the mean number of surface points with a specified slope $h_x = \beta$, given by

$$N_s(\beta) = \int_{-\infty}^{\infty} p(\xi_x, \xi_{xx})_{\xi_x=\sigma k\beta}|\xi_{xx}|d\xi_{xx} = k^4\sigma^2\int_{-\infty}^{\infty} p(h_x, h_{xx})_{h_x=\beta}|h_{xx}|dh_{xx}, \qquad (35)$$

where $p(\xi_x, \xi_{xx})$ and $p(h_x, h_{xx})$ are joint probability distributions of values ξ_x, ξ_{xx} and h_x, h_{xx}. We express z_1 and z_2 in terms of h_x and h_{xx} in the second-order approximation with respect to small δ (when $N = 1$),

$$z_1 = -h_{xx} - 2\delta h_{xx}^2 + 2\delta h_x^2, \qquad z_2 = -h_x - 2\delta h_x h_{xx} \qquad (36)$$

and pass from variables z_1 and z_2 to h_x and h_{xx} in (31). Then we have Substituting (37) into (35) and integrating with the use of steepest descent, the mean number of points of a given slope $h_x = \beta$ per unit length is written as

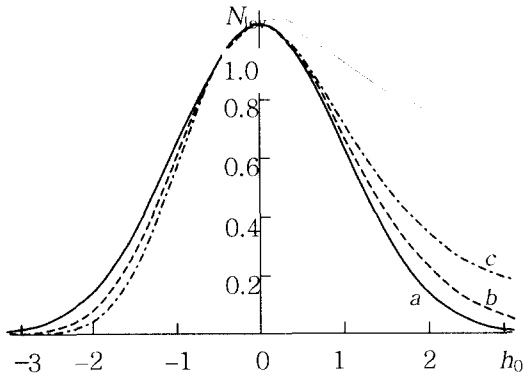

Fig. 10 Dependencies $N_{lev}(h_0,e)$ for various e

$$p(h_x, h_{xx}) = \frac{1}{2\pi}\exp\left(-\tfrac{1}{2}h_x^2 - 2\delta^2 h_x^4\right)\left|1 + 6\delta h_{xx}\right|\exp\left(-\tfrac{1}{2}h_{xx}^2 + 2\delta h_{xx}^3 + 2\delta^2 h_{xx}^4 - 2\delta^2 h_x^2 h_{xx}^2\right). \tag{37}$$

$$N_s(\beta,\delta) = \frac{k}{2\sqrt{\pi}}\exp\left(-\tfrac{1}{2}\beta^2 - 2\beta^4\delta^2\right)\left\{\begin{array}{l}\exp\left(-\tfrac{1}{2}+11\delta^2\right)\left[\begin{array}{l}\left(1+3\delta-71\delta^2+2\beta^2\delta^2\right)e^{-5\delta} \\ +\left(1-3\delta-71\delta^2+2\beta^2\delta^2\right)e^{5\delta}\end{array}\right] \\ +12\delta\exp\left(-1+44\delta^2\right)\left[\begin{array}{l}\left(1+6\sqrt{2}\delta-124\delta^2+4\beta^2\delta^2\right)e^{-10\sqrt{2}\delta} \\ -\left(1-6\sqrt{2}\delta-124\delta^2+4\beta^2\delta^2\right)e^{10\sqrt{2}\delta}\end{array}\right]\end{array}\right\} \tag{38}$$

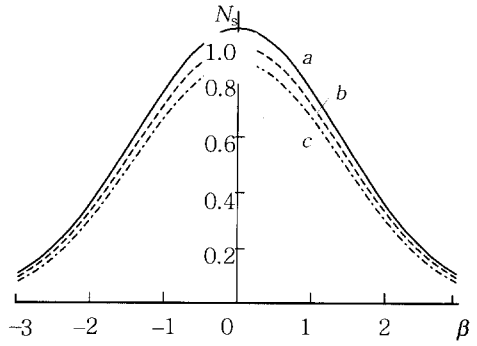

Fig. 11 Dependencies $N_s(\beta,e)$ for various $\delta = 2e$

Figure 11 shows dependencies $N_s(\beta,e)$ for various $\delta = 2e$. The case of $e = 0$ corresponds to the linear Gaussian surface. As the nonlinear parameter e grows, a deviation from the Gaussian model is observed, which consists in the $N_s(\beta,e)$ decrease compared to the linear case. The nonlinear effects are most pronounced for the density of mirror points with a quasizero ($\beta \approx 0$) slope. The relative deviation from the linear model can reach 10 % for quite moderate nonlinear parameters $e \sim 10^{-2}$, which makes it possible to observe nonlienar wave effects experimentally.

9. Conclusions

Remote sensing of the sea surface by a specularly reflected narrow laser beam opens wide opportunities to study statistical properties of the random sea. The models proposed allow one to investigate various spectral ranges of sea waves and, along with energy carrying long-wave components, to study behavior of high-frequency waves with a length of a few tens of centimeters. The technique implemented provides for reconstruction of parameters of the sea wave spatial spectrum using a single characteristic, that is the mean number of mirror laser specks per unit length at a few tacks of the flying laboratory.

The model of weakly nonlinear random surface allows one to trace the impact of nonlinearity on the wave statistics measured and to estimate deviation of the sea surface from the Gaussian random function.

The account of the mirror point velocity can substantially affect the wave angular parameters calculated and allows estimation of the velocity of energy carrying peak of the sea wave spectrum. Experimental determination of the variance in the mean number of mirror points on the interval of a given length opens the opportunity to build the surface correlation function without its preliminary parametrization.

Experiments on oblique laser remote sensing of the sea surface from an aircraft are perspective with a high-sensitive receiver (due to the expected poor statistics of specks). An important supplement to the laser technique considered is the phase profilometry that can be easily combined with the speck measurement. The possibility of direct determination of the mean wave height, that is the zero moment $m00$ of the sea directional spectrum, completely closes the problem of search for the spectrum free parameters.

Further development and application of the laser method proposed should result in reconstruction (by the statistics of mirror specks) of the total wave spatial energy spectrum and correlation function of the sea surface with no preliminary simulation.

Acknowledgement

The authors wish to acknowledge the financial support of the Korean Research Foundation made in the program year of 1999.

References

(1) Stamm G. and Harris L., Zakharov V.M., Pavlov V.N., and Rokotian V.E., "Trudy TsAO". Vol. 105, pp 69, 1973.

(2) Gurevich G.S., Zhiguleva I.S., Lysenko B.M.., "Optical Methods for Studying Oceans and Internal Water Bodies," pp 107, 1979a.

(3) Gurevich G.S., Zhiguleva I.S., Lysenko B.M., "Trudy TsAO". Vol. 139, pp 93, 1979b.

(4) Gurevich G.S., Proc. Symp. "On Laser Sounding of Atmosphere," pp 121, 1976.

(5) Goldin Yu.A, Kagain V.E., Kelbalikhanov B.F., and Pelevin V.N., "Optical Methods for Studying Oceans and Internal Water Bodies," pp 135, 1979.

(6) Pelevin V.N., "Light Fields in the Ocean," pp 212, Stemkovsky A.I., Ibid., pp 224, 1979.
(7) Ross D., Cardone V., and Conaway J., IEEE Trans. "Geosci. Electron". **8**(4), 326, 1970.
(8) Kulyasov A.G., Marasin L.E., Yu.V. Popov, Geodeziyai Kartografiya, No. 10, 41, 1979.
(9) Miller B., Aviat. "Week Space Technol". **82**(13), 60 1965.
(10) Olsen W. and Adams, Geophys J. Res. **75**(12), 2185 1970.
(11) Lin P. and Ross D., Phys J. Oceanogr. **10**(11), 1842 1980.
(12) Voliak K.I., Mikhalevich V.G., Shevchenko T.B., and Shugan V.I., Bull. Acad. Sci. USSR, Phys. Ser. **16**(10), 1111 1986.
(13) Bunkin F.V., Voliak K.I., Malyarovsky A.I., et al., "Oceanic Remote Sensing", pp 3, 1987.
(14) Bunkin F.V., Voliak K.I., Malyarovsky A.I., et al., Dokl. Akad. Nauk SSSR **281**, 1441 1985 (*Sov. Phys.-Doklady*).
(15) Grigoriev P.V., Shevchenko T.B., and Shugan I.V., Sov. Phys. Lebedev Inst. Rep. No. 5, 32, 1987.
(16) Huang N.E. and Long S.R., Fluid J. Mech. **101**, 179, 1980.
(17) Shevchenko T.B. and Shugan I.V., Sov. Phys. Lebedev Inst. Rep. No. 1, 9, 1988.
(18) Solntsev M.V., Sov. Phys. Lebedev Inst. Rep. No. 4, 22 1986.
(19) Longuet-Higgins M., Philos. Trans. R. Soc. London A **249**, 321, 1957.
(20) Rice S., Bell Syst. Tech. J. **23**, 282, 1944.
(21) Jansen P. and Komen G., J. Geophys. Res. **89**(3), 3635 1984.
(22) Phillips O.M., "The Dynamics of the Upper Ocean" (Wiley, N.Y.) pp 44, 1966.
(23) Cramer H. and Ledbetter M.R., "Stationary and Related Stochastic Processes" (Wiley, N.Y.,) pp 78, 1976.
(24) Steiberg H., Schultheiss P., Worgin C., and Zweig F., J. Appl. Phys. **26**, 195, 1966.
(25) Longuet-Higgins M., Fluid J. Mech. **17**, 459, 1963.
(26) Taifun M.A., Geophys J., Res. **85**, 1980.